

Global patterns of rain-on-snow and its impacts on runoff from past to future projections

Received: 7 November 2024

Fadji Z. Maina^{1,2}✉ & Sujay V. Kumar¹

Accepted: 2 May 2025

Published online: 21 May 2025

 Check for updates

Global warming has induced rain-on-snow (ROS) in cold regions leading to significant consequences on ecosystems and socioeconomic development. However, a global analysis of ROS under historical conditions and future projections following different emissions scenarios, essential for management strategies, is currently lacking. Here, we examine ROS changes and their impacts on the water available for runoff, analyzing historical conditions since 1950 and projecting future trends under SSP245 and SSP585 until 2100. By the end of the century, ROS will predominantly occur in high-latitude and altitude regions such as High Mountain Asia, the Alps, Northern Eurasia, and America with rates up to three times higher than those of the historical conditions. Nonetheless, the increasing rainfall will reduce by more than half the contribution of ROS to the water available for runoff despite its rise. Although regions like the Western United States have historically experienced significant ROS, warming will diminish ROS impacts as they become twice lower due to decreasing snowpack and intensified rainfall.

In cold regions, warming causes a shift in the precipitation phase from snow to rain, which falls over the snowpack and induces rain-on-snow (ROS). Over the past decades, ROS has been reshaping the hydrology of many cold regions, such as the Western United States (US), Europe, and Asia^{1–4}. Because ROS causes considerable and devastating hazards such as floods^{1,5}, avalanches, and acceleration of permafrost that lead to long-term structural instability⁶ and has serious consequences on infrastructure (e.g., the failure of the Oroville dam¹) and wildlife by forming ice barriers that prevent access to food, leading to starvation and mass die-offs⁷; it has been widely studied in many regions around the world using different methods and approaches. For instance, Cohen et al.⁸, studied ROS in the northern hemisphere, in particular in Western Eurasia, Western North America, the Northeastern US, and Southeastern Canada. ROS has also been studied over the Asian continent^{2,9–11}, Europe^{3,12–19}, Arctic^{20,21}, Canada^{22,23}, Alaska²⁴ and the continental US^{1,4,5,25–28}. These studies have shown that ROS consequences are complex and include floods, snow avalanches, soil erosion, and sediment transportation, which can lead to landslides and geomorphological changes^{25,29–31}. As the Earth's temperature continues to

increase in response to anthropogenic climate change, ROS is expected to change and significantly contribute to changing the hydrologic cycle of cold regions¹. Despite its significant importance for water management and ecosystems, ROS is still not completely understood in hydrology, and as such, it was highlighted among the twenty-three major unsolved hydrological problems³². Studies have demonstrated that ROS, by introducing warm rainfall in the snowpack, intensifies snow melting, further contributing to (1) the decline of the snowpack and (2) altering the snow dynamics such as destabilizing the snowpack in addition to reducing its cohesiveness, as well as altering the duration of the snowpack and the timing of snowmelt, causing it to occur more quickly^{33,34}. The impacts of ROS extend beyond the cold season, as the changes in the snow dynamics can (1) induce snow droughts, (2) affect the runoff not only in winter but also in spring and late summer, and (3) influence the availability of the groundwater and its recharge^{8,34–36}.

Future projections of ROS and its impacts on hydrology in particular runoff are difficult to quantify because of the complexity of the factors influencing ROS^{8,33,36}. For example, many factors that are region-dependent control the occurrence of ROS, such as the air temperature,

¹NASA Goddard Space Flight Center, Hydrological Sciences Laboratory, Greenbelt, MD, USA. ²University of Maryland, Baltimore County, Goddard Earth Sciences Technology and Research Studies and Investigations, Baltimore, MD, USA. ✉e-mail: fadji@maina.nasa.gov

the rainfall, and the snowpack on the ground. Similarly, the impacts of ROS may also depend on factors such as the state of the snowpack (i.e., wet or dry) and its thickness³³. Indeed, ROS will have a greater impact on a wet snowpack than a thick snowpack with a very low temperature because the rainfall will easily penetrate a wet snowpack and exacerbate its melting³³. In addition, the impacts of ROS in a given region depend on (1) its land cover, as ROS can impact vegetation growth and greenness and change the soil temperature, and (2) its topography because of the dependence of the longwave and shortwave components of the net radiation critical to snow dynamics on the topography^{7,12,28,37,38}. Therefore, ROS analyses cannot be generalized across regions, and the changes in ROS within each region must be studied. Consequently, a comprehensive global study of ROS and its impacts on runoff is essential to fully understand their dynamics across different regions. Such a study, despite being essential to providing a better understanding of the global dynamics of ROS as well as their particularities depending on the region, is currently lacking. Further, given that ROS caused by global warming is likely to change with the intensification of human-induced climate change, it becomes even more important to study these effects in future climates, while considering multiple pathways of greenhouse gas emissions. For example, in the Western US, Musselman et al.¹ and Li et al.²⁸ have studied the changes in ROS and their impacts on the runoff by the end of the century. Also, Myers et al.³⁹ projected the changes in ROS and their impacts on the runoff by mid-century over the Great lakes basins in North America, and Beniston et al.⁴⁰ projected the changes in ROS and their impacts on the runoff in the European Alps. Nonetheless, these studies remain region-specific (mostly focused on the US) and some only project ROS through the mid-century (i.e., 2050) rather than to the end of the century (i.e., 2100), when the hydrologic cycle will become more intense, although this period is associated with greater uncertainty.

In this study, we conduct a global assessment of ROS for both historical conditions and future projections using the Coupled Model Intercomparison Project Phase 6 (CMIP6). CMIP6 offers a standardized framework with coupled global climate models, providing a broad understanding of climate dynamics and interactions between the atmosphere, oceans, and land^{41–43}. Specifically, we investigate the ROS evolution by the end of the century under two greenhouse gas emissions scenarios: (1) SSP245 with an additional radiative forcing of 4.5 W/m² by the end of the century, representing the medium pathway of future greenhouse gas emissions; and (2) SSP585 with an additional radiative forcing of 8.5 W/m² by the end of the century, representing the upper boundary of the range of scenarios described in the literature. While the SSP245 scenario assumes that climate protection measures are being taken, the SSP585 scenario, similar to the Coupled Model Intercomparison Project Phase 5 (CMIP5) scenario RCP8.5, represents the most pessimistic scenario where the increase in greenhouse gas emissions will be the highest. We perform land surface model simulations, specifically, we use the Noah-MultiParameterization (Noah-MP⁴⁴) model, along with downscaled and bias-adjusted ensemble CMIP6 surface meteorology, to simulate the snow dynamics and hydrodynamics. This allows us to assess the impacts of ROS on the hydrology, particularly the runoff. Our results suggest that even though the two main meteorological drivers of ROS (i.e., precipitation and temperature) have been increasing in the historical period, ROS depicted a bidirectional pattern with an increasing trend in high latitude and altitude regions such as the European Alps, High Mountain Asia (HMA), High-Latitude North America, and Northern Eurasia and decreasing trends in low altitude regions such as some areas of the Western US and Eastern and Western Europe. While the direction of the trends in ROS remains the same under future projections (though it will intensify under global warming, especially under SSP585), the contribution of ROS to runoff decreases in many areas towards the end of the century, despite the fact that ROS is increasing and has significantly contributed to runoff during the historical period. As such, by the end of the century, rainfall intensity is projected to increase and will far exceed not only the snowmelt but also

the snowmelt resulting from ROS. These results suggest that by the end of the century, rainfall will likely cause more flood-related damages than ROS, despite ROS being more frequent in historical conditions, due to the disappearance of the snowpack caused by warming.

Results

Global patterns of ROS and its contributions to runoff under historical conditions

ROS generally occurs in the mountainous regions of the northern hemisphere (Fig. 1a, d, g) as highlighted in previous studies^{1,4}. In the southern hemisphere, only the Andes are subject to ROS (Fig. 1a) with magnitudes ten times lower than the average northern hemisphere ROS. 10 regions with noteworthy ROS activities can be distinguished: the High-Latitude North America, the Western US, the Rockies, the Eastern US, the Andes, Western Europe, the European Alps, Eastern Europe, Northern Eurasia, and HMA (Fig. 1j). Regions with significant amounts of ROS (more than 10% of the annual precipitation locally, as shown by the ratio of ROS to total precipitation in areas with red to dark-red color in Fig. 1d) during the historical period are also the ones discussed in the literature: the Western US^{1,28}, European Alps^{16,40}, HMA^{2,11}, and the Western part of High-Latitude North America²⁶. In these regions, over 30 days in the year identified as ROS days (i.e., the total number of days where ROS occurs, Fig. 1g). Note that these patterns are consistent with the conclusions of the aforementioned studies. In the Eastern US and Western and Eastern Europe, ROS represents less than 5% of the annual precipitation. Although Northern Eurasia is characterized by high snow depth, ROS is very low in the regions due to the relatively low rainfall, even in the summer.

Figure 2 illustrates the spatial distributions of the trends in ROS, temperature, precipitation, liquid precipitation (i.e., rainfall), and snow depth under both historical conditions and future projections. The trends in ROS over the historical period are shown in Fig. 2a. ROS is characterized by both increasing and decreasing trends, even if both total precipitation and temperature have increasing trends (Fig. 2d, g). Increasing trends in precipitation and temperature, in general, may lead to increasing trends in ROS, as the shift in precipitation phase caused by changes in temperature will lead to more rain falling on snow (as indicated by the trends in rainfall in Fig. 2j). However, ROS decreases because, in some areas, snow depth becomes very low or even non-existent (as shown by the decreasing trend in snow depth in Fig. 2m), as such, rain is no longer being deposited on snow. Such behavior is generally observed over the low-elevation regions of the Western US (note that ROS increases in high-elevation areas of this region, see Supplementary Fig. 1) as mentioned by Musselman et al.¹. Similar patterns are also observed in the Eastern US, and Western and Eastern Europe (Fig. 2a) as highlighted by Beniston et al.⁴⁰. Despite the Andes' high elevation (>1000 m, see Supplementary Fig. 2), ROS shows a decreasing trend due to decreasing trends in precipitation (and, therefore, rainfall, Fig. 2j). High latitude areas (latitude greater than 50°) are characterized by increasing trends in ROS, also reported in previous regional studies^{6,25,31}. In these areas, the precipitation (as well as liquid precipitation or rainfall) is increasing, which leads to more rain falling on snow, and the latter remains substantial despite the increasing temperature. Similar patterns are also observed in high-altitude regions such as the Alps and HMA, where persistent snowpack combined with increasing rainfall results in more ROS, as demonstrated in many studies^{2,16,45}.

In the northern hemisphere during the historical period, ROS significantly contributes to the water available for runoff, with the ratio of the snowmelt following ROS (QSM_{ROS}) to the water available for runoff defined as the sum of snowmelt and rainfall ($Runoff_{WA}$) $QSM_{ROS}/Runoff_{WA}$ reaching up to 0.3 over the Alps, HMA, Eastern and Western High-Latitude North America, Western US, and sparse areas in Northern Eurasia (Fig. 3a). In the Andes, the Eastern US, and Eastern Europe, the contribution of ROS to the water available for runoff is low (with the ratio $QSM_{ROS}/Runoff_{WA}$ inferior to 0.1), due to its low

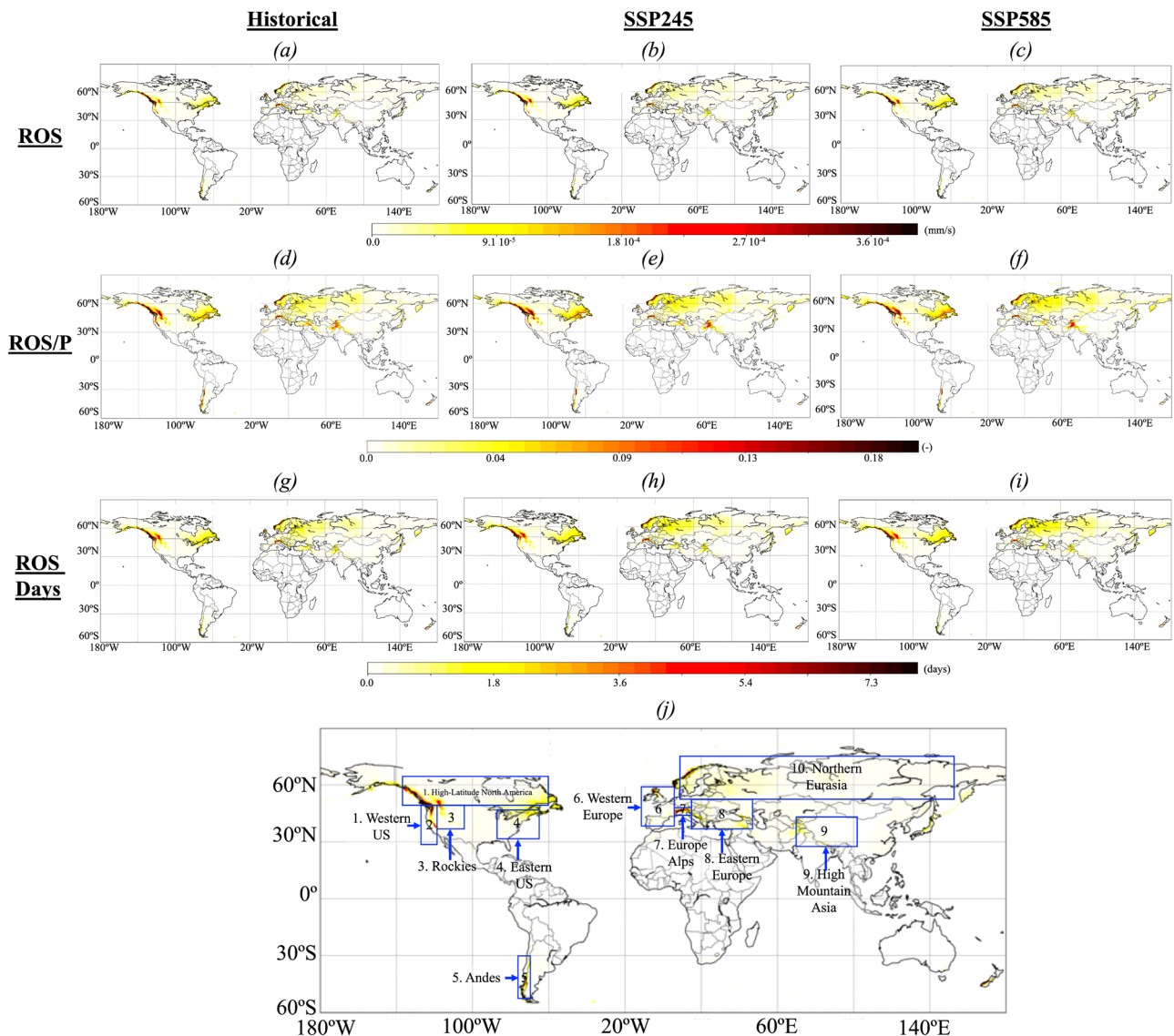


Fig. 1 | Rain-on-snow occurs most frequently in high-altitude and high-latitude regions, reaching up to 10% of annual precipitation. Spatial distributions of the annual average rain-on-snow (ROS) under a historical conditions (1950–2014), **b** SSP245 (2015–2095), and **c** SSP585 (2015–2095). The ratio of ROS to precipitation (ROS/P) is shown for **d** historical, **e** SSP245, and **f** SSP585 conditions, and the

number of ROS days (total days with ROS) is presented for **g** historical, **h** SSP245, and **i** SSP585 conditions. The black lines represent country boundaries. **j** highlights regions with significant ROS activity, with background shading indicating the historical annual average of ROS. See Supplementary Fig. 3 for differences between future and historical conditions. US is for United States.

occurrence in these regions, however, the snowmelt has a high contribution (greater than 0.5) to the water available for runoff (Fig. 3d).

Although the overall contribution of snowmelt to the water available for runoff (i.e., the sum of rainfall and snowmelt) decreases over the historical period (Fig. 4d) due to reduced snow and increased rainfall, the contribution of ROS to the water available for runoff continues to rise (Fig. 4a). While ROS events have declined in some areas, they still trigger intense snowmelt where they occur, given the increased vulnerability of a wet and thinning snowpack. As a result, ROS remains a significant contributor to the water available for runoff, as discussed in previous studies^{3,28,46}.

Global patterns of ROS and its contributions to the water available for runoff under future projections (SSP245 and SSP585)

Under future projections (in SSP245 and SSP585), areas subject to ROS are similar to those under historical conditions (Fig. 1b–d, h, i). However, ROS/P is generally lower under future projections than during the

historical period in low-latitude zones of the northern hemisphere and higher in high-latitude (greater than 50°) regions (Supplementary Fig. 3). The two future projection scenarios differ in the total amount of ROS (as shown in Supplementary Fig. 3), SSP245 shows more ROS magnitude and days (with the ratio of ROS to precipitation being up to 0.2 greater than that of SSP585) in low elevation areas, whereas SSP585 has more ROS amount and days (with the ratio of ROS to precipitation being up to 0.1 greater than that of SSP245) in high latitude and altitude regions. Similar to the averages, the trends in ROS under the historical periods and the future projections have similar spatial patterns (Fig. 2b, c). However, the magnitudes of the trends are higher in future projections because of the intensification of the hydrologic cycle under global warming as highlighted in the IPCC reports^{47,48}. The trends are more pronounced in SSP585 than in SSP245, whose trends are higher than those of the historical conditions. Changes in precipitation and temperature are significant under SSP585 (Fig. 2f, i) compared to SSP245 (Fig. 2e, h), hence changes in ROS are considerable. In both scenarios, ROS is projected to increase in high latitudes

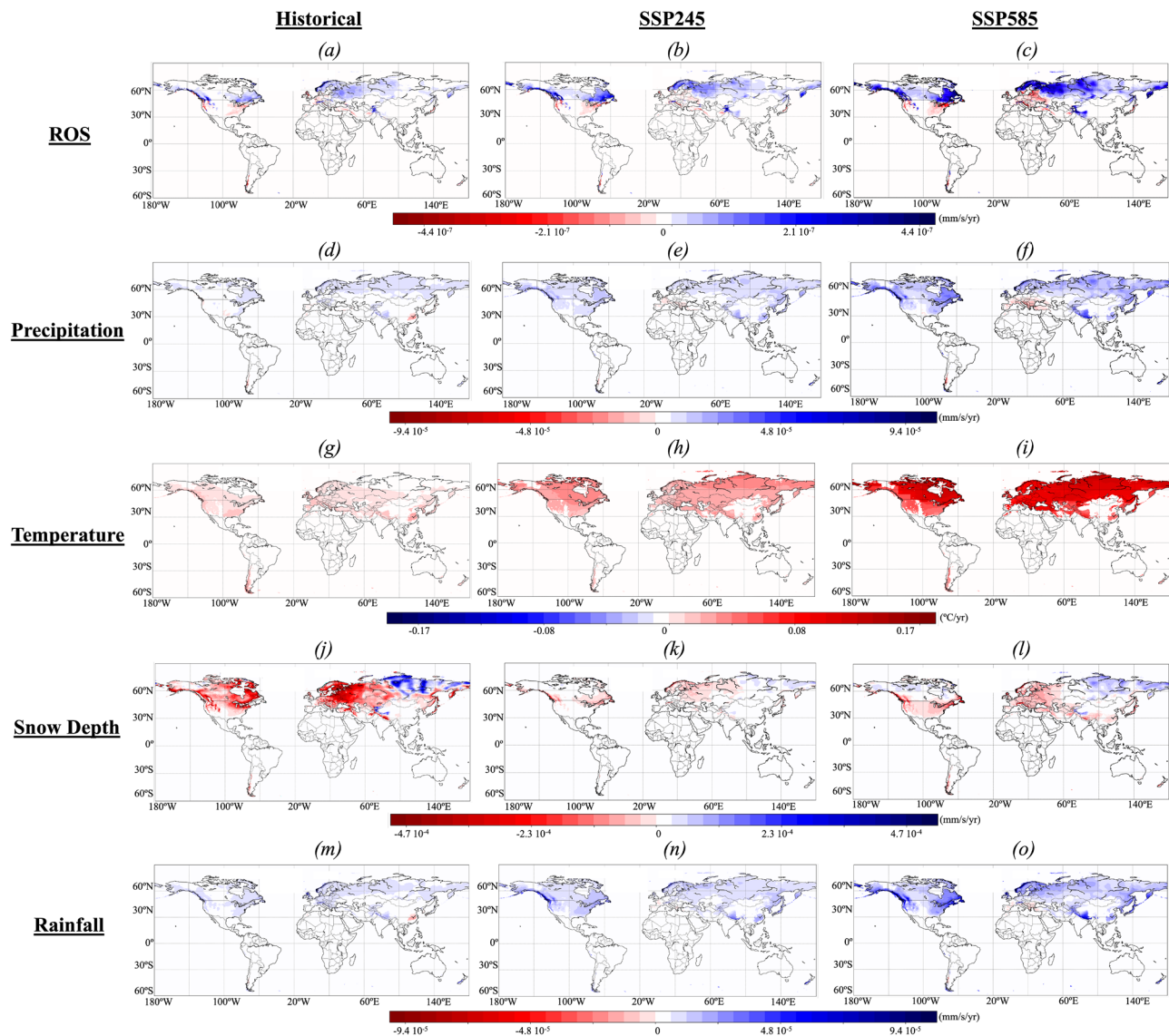


Fig. 2 | Declining trends in rain-on-snow at mid-elevations and mid-latitudes, while increases are observed in high-altitude and high-latitude regions. Spatial distributions of trends in a–c rain-on-snow (ROS), d–f temperature, g–i precipitation, j–l liquid precipitation, and m–o snow depth under a, d, g, j, m historical conditions (1950–2014), b, e, h, k, n SSP245 (2015–2095) and c, f, i, l, o SSP585 (2015–2095).

(i.e., greater than 50°) due to the shift in precipitation from snowfall to rainfall, in addition to the increase of the latter (Fig. 2k, l). During the historical period, the other regions are characterized by bidirectional trends, where the low elevations have decreased trends and the high elevation regions see an increase. In the Western US and the Rockies, some areas have increasing trends in ROS in the historical period and decreasing trends in the future projections due to the reductions of the snowpack (Fig. 2n, o). Precipitation is generally projected to increase on Earth in the future (Fig. 2h, i), however, most of Europe will experience a decrease in precipitation under both SSP245 and SSP585. This will also translate into a decrease in rainfall mostly observed over Western Europe and localized areas of Eastern Europe (Fig. 2k, l). Note that decreasing trends in precipitation in Europe have been highlighted in the latest IPCC's Sixth Assessment Report⁴⁹. Despite experiencing decreases in precipitation, the Alps, as well as many areas of Europe characterized by high elevation, have an increasing trend in ROS because the rainfall increases (Fig. 2k, l) consistent with previous studies^{16,40}.

The spatial patterns of ROS contributions to the water available for runoff in future projections are similar to those observed

historically, with the highest contributions occurring in high-latitude and high-altitude regions (Fig. 3b, c). ROS significantly impacts the water available for runoff in areas where snowmelt plays a substantial role, particularly in High-Latitude North America, the Alps, and HMA, where the $QSM_{ROS}/Runoff_{WA}$ ratio exceeds 0.35 (Fig. 3e, f). Over the Andes, ROS contributions to the water available for runoff are negligible, despite snowmelt's notable impact on the water available for runoff in that region and in most of Europe outside the Alps (Fig. 3e, f).

Historically, the contributions of the snowmelt triggered by ROS to the water available runoff have increased (Fig. 4a), but they are projected to decline (with the ratio of $QSM_{ROS}/Runoff_{WA}$ decreasing by more than 0.005 in many areas) in the future (Fig. 4b, c), particularly in areas such as the Western U.S., where decreases or even an absence of ROS are expected, aligning with the findings of Musselman et al.¹. This is due to the decreasing occurrence of ROS and the increasing rainfall caused by warming, which falls directly on the ground rather than on snow. Only the HMA and some high-latitude regions are expected to see a slight increase in ROS-related runoff. Furthermore, ROS contributions are higher under SSP585 than SSP245, owing to greater ROS intensity in SSP585 (Fig. 3b, c, Supplementary Fig. 3).

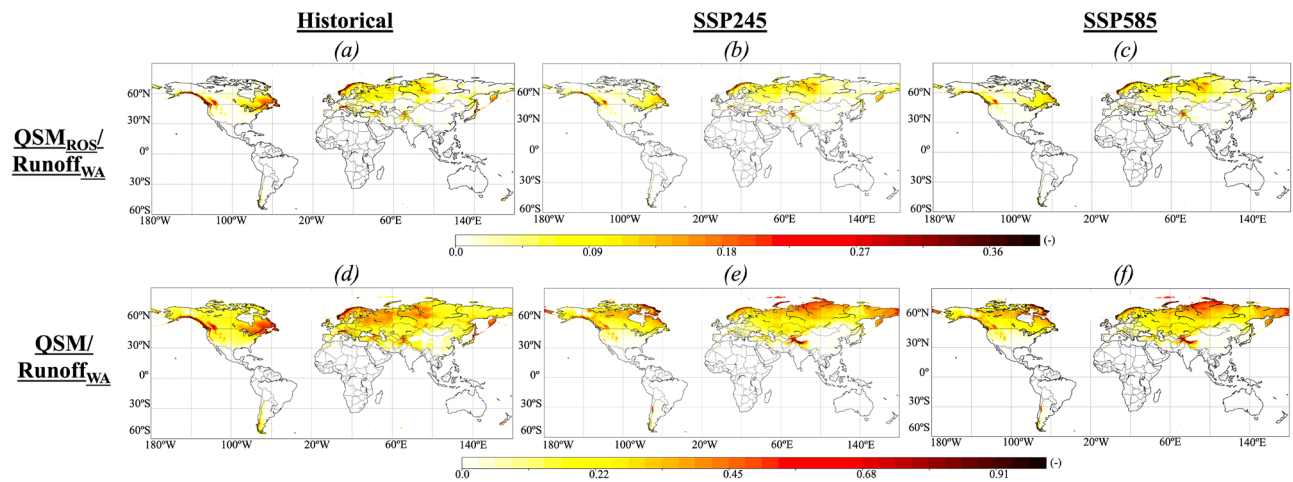


Fig. 3 | Significant contribution of rain-on-snow to runoff generation in mountainous areas. Spatial distributions of the annual average ratio of snowmelt following rain-on-snow (ROS) referred here as QSM_{ROS} to total water available for runoff ($Runoff_{WA}$: liquid precipitation + snowmelt) under (a) historical conditions (1950–2014), (b) SSP245 (2015–2095), and (c) SSP585 (2015–2095); and the ratio of total snowmelt (QSM) to $Runoff_{WA}$ under (d) historical conditions, (e) SSP245, and (f) SSP585.

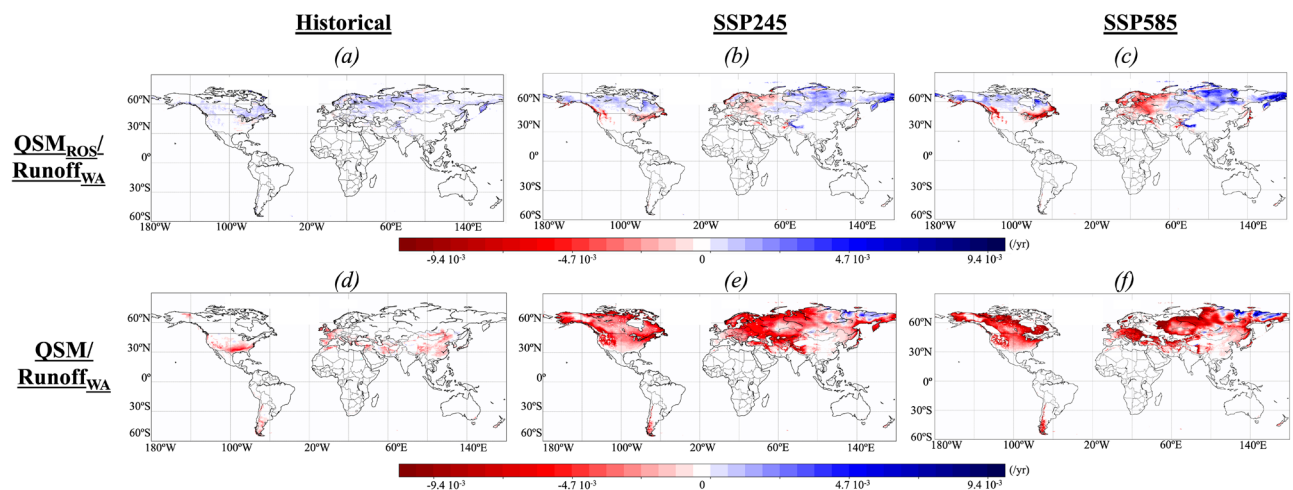


Fig. 4 | Although historically significant, rain-on-snow contributions to water available for runoff are projected to decline in many regions by the end of the century. Spatial distributions of trends in the ratio of snowmelt following rain-on-snow (ROS) referred here as QSM_{ROS} to total water available for runoff ($Runoff_{WA}$: liquid precipitation + snowmelt) under a historical conditions (1950–2014), b SSP245 (2015–2100), and c SSP585 (2015–2095); and in the ratio of total snowmelt (QSM) to $Runoff_{WA}$ under d historical, e SSP245, and f SSP585 conditions.

Historically, the contribution of ROS to the water available for runoff rose despite a decrease in snowmelt contributions, largely due to a modest increase in rainfall. By the end of the century, however, a dramatic rise in rainfall is anticipated, likely exceeding snowmelt, including that driven by ROS, in its contribution to the water available for runoff (Fig. 4d–f). Consequently, while ROS may increase in some regions, the more intense rise in rainfall suggests that severe floods are likely to be driven by rainfall alone, potentially reducing the relative impact of ROS.

Regional dynamics of ROS and its contribution to the water available for runoff

An analysis of the monthly variations of ROS over the regions highlighted in Fig. 1j shows that depending on the region, ROS can occur (1) in December and January in areas with low snowpack and relatively low latitude and elevation such as the Western US, Eastern and Western Europe, and the Andes, (Fig. 5 and Supplementary Fig.) and (2) mostly in March in high latitude and altitude regions such as High-Latitude North America, the Alps, Northern Eurasia, and HMA (Fig. 6 and Supplementary Fig. 5).

Regions where the highest ROS (more than 10% of the annual precipitation) occurs in January and December are characterized by a decreasing trend in ROS in both historical conditions and future projections (up to 0.2 mm/d/year) as shown in Fig. 5. As previously noted, this decrease is more pronounced in SSP585 than in SSP245. In these regions, ROS occurs in January and December because (1) of the presence of snow and (2) the shift in precipitation phase mostly occurs during that time. In late winter, because of warming, though the precipitation is mostly in the form of rainfall than snowfall, the snow is so scarce for the rainfall cause ROS; the latter falls on the ground. These regions are also characterized by a decrease in the contribution of ROS to the water available for runoff by the end of the century (as indicated by the ratio $QSM_{ROS}/Runoff_{WA}$ in Fig. 5). Such a decrease in the contribution of ROS to the water available for runoff under future projections (by more than 65% of its historical values) is more pronounced than the decreasing trend in ROS (which decreases by ~50%) because of the increase in rainfall.

The majority of ROS occurs in March in high latitude and altitude regions because, in these regions, though the precipitation shifts from

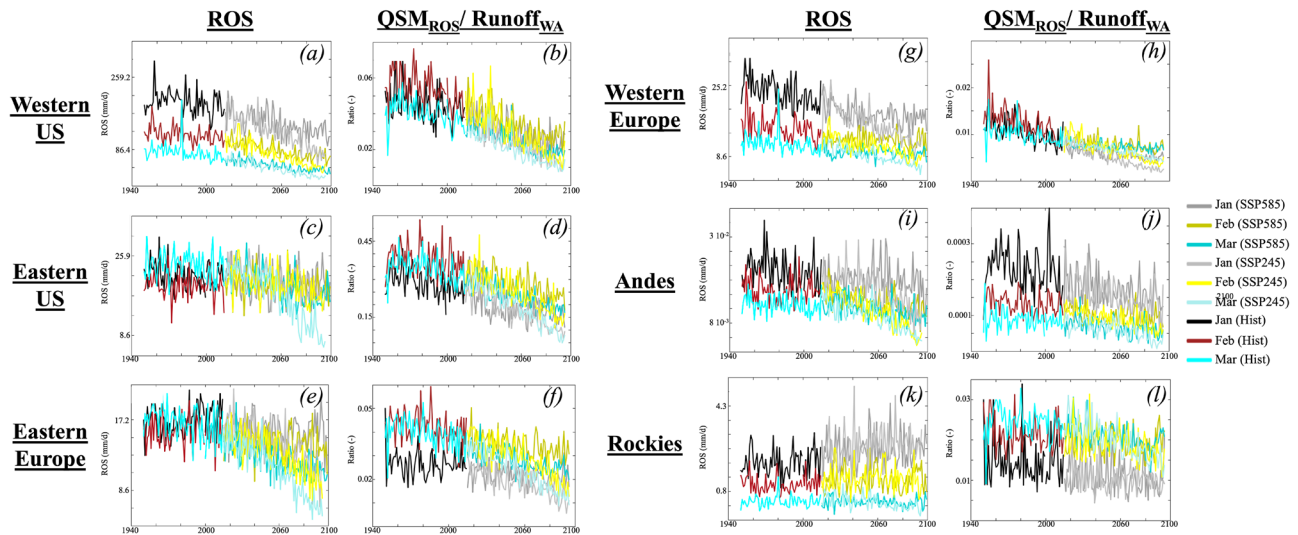


Fig. 5 | In some regions, both rain-on-snow and its contribution to water available for runoff are decreasing. Yearly averages of rain-on-snow (ROS) and the ratio of snowmelt following ROS referred here as QSM_{ROS} to total runoff ($Runoff_{WA}$:

liquid precipitation + snowmelt) from January to March under historical and future projections for regions in Fig. 1j: **a, b** Western US, **c, d** Eastern US, **e, f** Eastern Europe, **g, h** Western Europe, **i, j** Andes, and **k, l** Rockies.

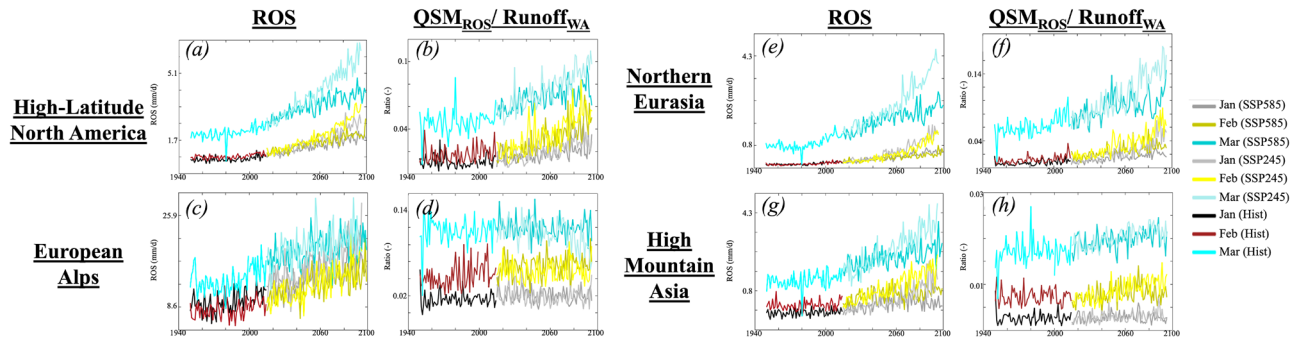


Fig. 6 | In high-latitude and high-altitude areas, Rain-on-Snow (ROS) and its contribution to water available for runoff are showing an increasing trend. Yearly averages of rain-on-snow (ROS) and the ratio of snowmelt following ROS referred here as QSM_{ROS} to total runoff ($Runoff_{WA}$: liquid precipitation + snowmelt)

from January to March under historical conditions and future projections for regions in Fig. 1j: **a, b** High-Latitude North America, **c, d** European Alps, **e, f** Northern Eurasia, and **g, h** High Mountain Asia.

snowfall to rainfall, this mostly happens towards the end of the winter when the weather warms up (Fig. 6 and Supplementary Fig. 6). In January and February, warming is not significant enough to cause a remarkable shift in the precipitation phase. Under future projections, ROS increases for all months, however, the rate of increase is different from one month to another, and March has the highest increase because of its relatively high temperature compared to the other winter months. By the end of the century (notably under the SSP585 scenario), ROS will also have a significant occurrence in February, though March has the highest quantity. However, over the Alps, while in the historical period, the highest ROS occurs in March, toward the end of the century, the quantity of ROS in March is similar to that occurring in January and February in particular under the SSP585 scenario. Changes in the contribution of ROS to the water available for runoff are not significant compared to those of ROS. In high latitudes (i.e., High-Latitude North America and Northern Eurasia), the contribution of ROS to the water available for runoff increases since, in these regions, the shift in the precipitation phase is not significant enough to make rainfall the dominant driver of the water available for runoff and mostly happens in March. Besides, the snowpack in these areas is considerable and less vulnerable to the high snowmelt triggered by ROS. In the Alps and HMA, the high increases in ROS do not induce a noteworthy increase in its contribution to the

water available for runoff because the increase in rainfall outweighs that of ROS. In these regions, future floods will likely be induced by the intensification of rainfall rather than ROS.

Discussion

This study presents a global quantification of ROS and their drivers using simulations from a land surface model (Noah-MP) based on CMIP6 datasets. The simulations were conducted at a higher spatial resolution than the original CMIP6 datasets, allowing for a more detailed analysis of the impacts of ROS. However, we acknowledge that a 10-km resolution may still be too coarse to accurately capture snow dynamics especially in mountainous regions^{50,51}. Future studies could downscale these models to better reproduce snow dynamics. Additionally, because these models are computationally expensive, requiring several months to complete a single simulation, and data processing is also time-intensive, it is impractical to run them with multiple parameterizations for a comprehensive sensitivity analysis and uncertainty quantification.

Overall, our results are consistent with previous studies performed at regional scales, that have shown the increasing trends in ROS in Western USA^{1,39} (during both the historical and the future projections) and the eastern HMA^{2,11}, and its decreasing trends in Europe⁵². The decreasing ROS in low elevation zones and its increase in high elevation areas have also been highlighted in previous studies³⁹.

Such changes in ROS are the result of the changes in precipitation patterns and temperature as projected by the CMIP6 models^{42,53}.

ROS is most common in the Northern Hemisphere, while in the Southern Hemisphere, only the Andes experience ROS, and even then, at very low magnitudes. As global temperatures rise, ROS are expected to shift toward higher latitude and altitude zones, increasing hazards and impacts on communities and ecosystems. In mid-latitude and mid-altitude regions, i.e., western US and Europe, ROS, which primarily occurs in January, has historically contributed to the water available for runoff but is projected to decrease in the future. Consequently, the water available for runoff in these regions will be dominated by rainfall rather than snowmelt, including that triggered by ROS. A decline in ROS could significantly impact water availability, as ROS has traditionally contributed substantially to runoff and recharge groundwater in the western U.S. and Europe in particular in spring^{1,2,4}. With more rainfall coming to the ground, such runoff will be instantaneous. Additionally, the reduction in ROS, coupled with diminished snowpack, could exacerbate summer hydrological droughts⁸. Most precipitation will likely fall as rain in limited periods, leaving much of the year without sufficient snowmelt or precipitation to replenish water systems. This change could be especially severe for regions like the western U.S., where snow has historically been the primary source of freshwater. In mountainous regions of the Earth's lower temperate zone, such as the Alps and HMA, ROS has historically occurred in March and is expected to increase under both SSP245 and SSP585 scenarios. By the end of the century, ROS is also projected to occur more frequently in February. However, despite the increase in ROS, its contribution to the water available for runoff is not expected to rise significantly because more intense rainfall is likely to cause greater damage than the increase in ROS. In high-latitude regions like Northern High-Latitude North America and Eurasia, ROS will continue to occur in March, with its contribution to the water available for runoff expected to increase since the shift from snow to rain is not significant enough for rainfall to overshadow the effects of ROS. The rising incidence of ROS in these high-latitude regions could have severe consequences for wildfires, infrastructure, and communities⁶.

Globally, as more precipitation falls as rain rather than snow, rainfall-induced floods can far surpass the magnitude of typical snowmelt-driven floods⁵⁴. Consequently, warming is likely to reduce the impact of ROS as it becomes less frequent, with other factors like rainfall dominating the water available for runoff. This makes adaptation to rainfall-induced floods crucial. As rainfall and ROS increase, the snowpack decreases, making it more vulnerable to ROS. In this phase, any ROS can trigger significant snowmelt, further depleting the snowpack until it eventually disappears, leading to a scarcity of ROS. The hydrological impact of ROS is greatest during the intermediate stage of snowpack decline, before it disappears completely. Therefore, additional management strategies are needed to address the effects of ROS in mid-latitude and high-altitude regions, which are expected to undergo this transition. By the end of the century, regions like the Alps and HMA are projected to experience shifts in the timing of ROS, affecting water resource management. Early ROS in these areas will further reduce snowpack and late-season snowmelt, which are vital for recharging groundwater and rivers. This shift could lead to a summer hydrological drought and impact water availability. However, regions such as HMA (notably over the eastern Karakoram), the Alps, Northern Eurasia, and High-Latitude North America are unlikely to reach the critical point where the snowpack becomes so rare that ROS diminishes by the end of the century. Additionally, their snowpack will not be as wet and thin as the snowpack of mid-latitude and altitude regions to exacerbate the consequences of ROS on the hydrology.

Methods

Our modeling was performed using the land surface model Noah-MP version 4.0.1⁴⁴. Within the NASA Land Information System (LIS⁵⁵). The

Noah-MP physically simulates key land surface processes and land-atmosphere interactions and has been widely used in the community^{44,56–58}. The model enables the simulation of cold-season processes, including snow accumulation and melt. In addition, Noah-MP simulates the surface and subsurface hydrodynamics, enabling the computation of runoff and other hydrologic variables. The model simulations were conducted on a global domain at a spatial resolution of 0.1° and a temporal resolution of a day. Downscaled climate data from CMIP6 was used as meteorological boundary conditions within these model runs. Specifically, we employ the NASA Earth Exchange Global Daily Downscaled Projections (NEX-GDDP⁵⁹) dataset, which employs the Bias-Correction Spatial Disaggregation (BCSD⁶⁰) method using the Global Meteorological Forcing Dataset (GFMD⁶¹) as the reference to daily, 25 km resolution data products. We further employ a temporal disaggregation scheme to develop sub-daily estimates of meteorological data, to enable land surface simulations with Noah-MP. Daily and hourly climatology for each surface meteorology variable is computed using the NASA Modern-Era Retrospective analysis for Research and Applications (MERRA-2⁶²) data. The NEX-GDDP meteorological data is then disaggregated to hourly timescales as:

$$GDDP_h^i = GDDP_d^i * \frac{\overline{MERRA2_h^i}}{\overline{MERRA2_d^i}} \quad (1)$$

Where $GDDP_h^i$ and the $GDDP_d^i$ are the hourly and daily GDDP values of a given variable, respectively and $\overline{MERRA2_h^i}$ and $\overline{MERRA2_d^i}$ are the hourly and daily climatology of a given variable, for a certain day i .

Using this downscaled forcing data, we simulated the historical conditions (i.e., from 1950 to 2014) and the future projections using two scenarios: SSP245 representing the optimistic scenario and SSP585 representing the worst-case scenario. All model simulations (i.e., historical, SSP245, and SSP585) are conducted with 25 Global Circulation Models (GCMs indicated in Supplementary Table 1) employed in CMIP6.

The historical simulations were evaluated by comparing key variables essential for assessing ROS changes and their contributions to the water available for runoff, namely, precipitation, snow depth, and air temperature, against widely used global datasets: ERA5-Land⁶³, the Global Precipitation Measurement (GPM) Integrated Multi-satellite Retrievals for GPM (IMERG⁶⁴), MERRA-2⁶², and a global land reanalysis⁶⁵ called HydroGlobe (<https://ldas.gsfc.nasa.gov/hydroglobe>) that employs MERRA-2 and IMERG with other land remote sensing datasets. This reanalysis was specifically used to assess simulated snow depth, as MERRA-2 and IMERG primarily provide surface meteorological data and do not include snow depth. Comparisons were conducted over different time periods based on each dataset's availability: ERA5-Land was assessed over the full historical period (1950–2014), MERRA-2 from 1980 to 2014, and IMERG from 2001 to 2014. Given that our study primarily focuses on trend analysis, we evaluated whether the trends identified in our simulations align with those in these widely used datasets. As shown in Supplementary Fig. 7, our results are generally consistent with these datasets. For example, our model captures 79% of the positive precipitation trends from ERA5-Land (74% of the total grid cells), 48% from IMERG (69% of the total grid cells), and 71% from MERRA-2 (47% of the total grid cells). For negative precipitation trends, the capture rates are 37%, 64%, and 25% for ERA5-Land, MERRA-2, and IMERG, respectively. The lower capture rates for negative trends are due to their relative scarcity. For instance, only 26% of grid cells exhibit such trends in ERA5-Land. Snow depth and air temperature exhibit overall decreasing and increasing trends, respectively, which are well represented in our simulations. Specifically, 75% of the decreasing snow depth trends in ERA5-Land (where 75% of the cells have negative trends) are captured by our model, while this percentage is 67% for HydroGlobe (with fewer cells exhibiting negative trends compared to

ERA5, as HydroGlobe only covers recent years from 2003 to 2014). For air temperature, comparisons with ERA5-Land indicate that the increasing trend is captured (with a percentage of 91%, note that the percentage of the negative hit is 0% because all the snow-covered areas show an increasing i.e., positive trends).

We performed the ROS analysis on each of these ensembles, then averaged these quantities to compute the trends and the yearly averages. We acknowledge that the different models have varying levels of uncertainty and are not equivalent, whereas the simple averaging procedure assumes equal weighting. To assess the impact of this averaging approach, we compared the trend signs obtained from the ensemble mean to those of each individual ensemble member. Specifically, we evaluated trends in key variables critical to our study, as previously mentioned. The results, shown in Supplementary Fig. 8, indicate that the trend signs of the ensemble mean align with at least the majority of the individual ensemble members, with agreement reaching up to 80% in many regions. This consistency suggests that the ensemble mean effectively captures the general trends of the individual models and is suitable for analysis.

To be consistent with previous studies^{1,2}, we identified ROS day as a day when at least 10 mm of rainfall (i.e., total liquid precipitation during the day) falls on at least 10 mm of snowpack, though other studies have used different approaches to study ROS dynamics^{4,46}. Indeed, there are different definitions of ROS in the literature, however, most of the studies use thresholds for both rainfall and snowpack, yet these thresholds depend on the study region. To understand the contribution of ROS to the water available for runoff and better characterize its implications for floods, we quantified the ratio of the snowmelt following ROS (i.e., the snowmelt occurring a day after ROS) to the total water available for runoff, defined as the sum of total rainfall and snowmelt following these studies^{1,66,67}. For the historical conditions and the future projections, we computed their trends (in addition to other hydrologic variables such as precipitation, rainfall, snow depth, etc.) using the Mann-Kendall test. The Mann-Kendall test is a widely used statistical method in hydrology for detecting trends in hydrological variables over time^{68–70}.

To analyze the changes in ROS as well as its contribution to the water available for runoff over the historical determines whether a time series has a monotonic upward or downward trend^{70–72}. The trend is computed using the following:

$$S = \sum_{i=1}^{n-1} \sum_{j=k+1}^n \text{sign}(x_j - x_i) \quad (2)$$

where x is the time series variable. The subscript j and k are the observation time. $\text{sign}(x_j - x_i)$ is equal to +1, 0, or –1, which means increasing, no, and decreasing trends, respectively. In this study, we assumed that there is no significant trend in the data at 95% confidence level (or at a significant level of 5% i.e., p -values less than 0.05).

Data availability

The dataset used in this study can be found in Maina and Kumar, 2025⁷³.

Code availability

We used the NASA Land Information System (LIS, <http://lis.gsfc.nasa.gov>), which is a comprehensive land surface modeling and data assimilation framework that supports modeling over user-specified regional or global domains using an ensemble of land surface models. The code is publicly available on GitHub: <https://github.com/NASA-LIS>

References

- Musselman, K. N. et al. Projected increases and shifts in rain-on-snow flood risk over western North America. *Nat. Clim. Change* **8**, 808–812 (2018).
- Maina, F. Z. & Kumar, S. V. Diverging trends in rain-on-snow over high mountain asia. *Earths Future* **11**, e2022EF003009 (2023).
- Sui, J. & Koehler, G. Rain-on-snow induced flood events in Southern Germany. *J. Hydrol.* **252**, 205–220 (2001).
- McCabe, G. J., Clark, M. P. & Hay, L. E. Rain-on-Snow Events in the Western United States. *Bull. Am. Meteorol. Soc.* **88**, 319–328 (2007).
- Pradhanang, S. M. et al. Rain-on-snow runoff events in New York. *Hydrol. Process.* **27**, 3035–3049 (2013).
- Forbes, B. C. et al. Sea ice, rain-on-snow and tundra reindeer nomadism in Arctic Russia. *Biol. Lett.* **12**, 20160466 (2016).
- Wayand, N. E., Lundquist, J. D. & Clark, M. P. Modeling the influence of hypsometry, vegetation, and storm energy on snowmelt contributions to basins during rain-on-snow floods. *Water Resour. Res.* **51**, 8551–8569 (2015).
- Cohen, J., Ye, H. & Jones, J. Trends and variability in rain-on-snow events. *Geophys. Res. Lett.* **42**, 7115–7122 (2015).
- Ohba, M. & Kawase, H. Rain-on-Snow events in Japan as projected by a large ensemble of regional climate simulations. *Clim. Dyn.* **55**, 2785–2800 (2020).
- Whitaker, A. C. & Sugiyama, H. Seasonal snowpack dynamics and runoff in a cool temperate forest: lysimeter experiment in Niigata, Japan. *Hydrol. Process.* **19**, 4179–4200 (2005).
- Yang, T. et al. Trends and spatial variations of rain-on-snow events over the high Mountain Asia. *J. Hydrol.* **614**, 128593 (2022).
- Garvelmann, J., Pohl, S. & Weiler, M. Spatio-temporal controls of snowmelt and runoff generation during rain-on-snow events in a mid-latitude mountain catchment. *Hydrol. Process.* **29**, 3649–3664 (2015).
- Merz, R. & Blöschl, G. A process typology of regional floods. *Water Resour. Res.* **39**, 1340 (2003).
- Nied, M. et al. On the relationship between hydro-meteorological patterns and flood types. *J. Hydrol.* **519**, 3249–3262 (2014).
- Pall, P., Tallaksen, L. M. & Stordal, F. A climatology of rain-on-snow events for Norway. *J. Clim.* **32**, 6995–7016 (2019).
- Rössler, O. et al. Retrospective analysis of a nonforecasted rain-on-snow flood in the Alps – a matter of model limitations or unpredictable nature? *Hydrol. Earth Syst. Sci.* **18**, 2265–2285 (2014).
- Tarasova, L., Basso, S. & Merz, R. Transformation of generation processes from small runoff events to large floods. *Geophys. Res. Lett.* **47**, e2020GL090547 (2020).
- Ulbrich, U. & Fink, A. The January 1995 flood in Germany: meteorological versus hydrological causes. *Phys. Chem. Earth* **20**, 439–444 (1995).
- Wever, N., Jonas, T., Fierz, C. & Lehning, M. Model simulations of the modulating effect of the snow cover in a rain-on-snow event. *Hydrol. Earth Syst. Sci.* **18**, 4657–4669 (2014).
- Rennert, K. J., Roe, G., Putkonen, J. & Bitz, C. M. Soil thermal and ecological impacts of rain on snow events in the circumpolar Arctic. *J. Clim.* **22**, 2302–2315 (2009).
- Serreze, M. C. et al. Arctic rain on snow events: bridging observations to understand environmental and livelihood impacts. *Environ. Res. Lett.* **16**, 105009 (2021).
- Loukas, A., Vasilades, L. & Dalezios, N. R. Flood producing mechanisms identification in southern British Columbia, Canada. *J. Hydrol.* **227**, 218–235 (2000).
- Trubilowicz, J. W. & Moore, R. D. Quantifying the role of the snowpack in generating water available for run-off during rain-on-snow events from snow pillow records. *Hydrol. Process.* **31**, 4136–4150 (2017).
- Pan, C. G., Kirchner, P. B., Kimball, J. S., Kim, Y. & Du, J. Rain-on-snow events in Alaska, their frequency and distribution from satellite observations. *Environ. Res. Lett.* **13**, 075004 (2018).
- Bieniiek, P. A. et al. Assessment of Alaska rain-on-snow events using dynamical downscaling. *J. Appl. Meteorol. Climatol.* **57**, 1847–1863 (2018).

26. Il Jeong, D. & Sushama, L. Rain-on-snow events over North America based on two Canadian regional climate models. *Clim. Dyn.* **50**, 303–316 (2018).
27. Leathers, D. J., Kluck, D. R. & Kroczyński, S. The severe flooding event of January 1996 across North-Central Pennsylvania. *Bull. Am. Meteorol. Soc.* **79**, 785–798 (1998).
28. Li, D., Lettenmaier, D. P., Margulis, S. A. & Andreadis, K. The role of rain-on-snow in flooding over the conterminous United States. *Water Resour. Res.* **55**, 8492–8513 (2019).
29. Harr, R. D. Some characteristics and consequences of snowmelt during rainfall in western Oregon. *J. Hydrol.* **53**, 277–304 (1981).
30. Stemberis, J. & Rubin, C. M. Glide avalanche response to an extreme rain-on-snow event, Snoqualmie Pass, Washington, USA. *J. Glaciol.* **57**, 468–474 (2011).
31. Crawford, A. D., Alley, K. E., Cooke, A. M. & Serreze, M. C. Synoptic climatology of rain-on-snow events in Alaska. *Mon. Weather Rev.* **148**, 1275–1295 (2020).
32. Blöschl, G. et al. Twenty-three unsolved problems in hydrology (UPH) – a community perspective. *Hydrol. Sci. J.* **64**, 1141–1158 (2019).
33. Groisman, P. Y. et al. Trends in intense precipitation in the climate record. *J. Clim.* **18**, 1326–1350 (2005).
34. Putkonen, J. & Roe, G. Rain-on-snow events impact soil temperatures and affect ungulate survival. *Geophys. Res. Lett.* **30**, 1188 (2003).
35. Myers, D. T., Ficklin, D. L. & Robeson, S. M. Incorporating rain-on-snow into the SWAT model results in more accurate simulations of hydrologic extremes. *J. Hydrol.* **603**, 126972 (2021).
36. Putkonen, J. et al. Rain on snow: little understood killer in the North. *Eos Trans. Am. Geophys. Union* **90**, 221–222 (2009).
37. Garvelmann, J., Pohl, S. & Weiler, M. Variability of observed energy fluxes during rain-on-snow and clear sky snowmelt in a midlatitude mountain environment. *J. Hydrometeorol.* **15**, 1220–1237 (2014).
38. Pohl, S., Marsh, P. & Liston, G. E. Spatial-temporal variability in turbulent fluxes during spring snowmelt. *Arct. Antarct. Alp. Res.* **38**, 136–146 (2006).
39. Myers, D. T., Ficklin, D. L. & Robeson, S. M. Hydrologic implications of projected changes in rain-on-snow melt for Great Lakes Basin watersheds. *Hydrol. Earth Syst. Sci.* **27**, 1755–1770 (2023).
40. Beniston, M. & Stoffel, M. Rain-on-snow events, floods and climate change in the Alps: events may increase with warming up to 4 °C and decrease thereafter. *Sci. Total Environ.* **571**, 228–236 (2016).
41. O'Neill, B. C. et al. The Scenario Model Intercomparison Project (ScenarioMIP) for CMIP6. *Geosci. Model Dev.* **9**, 3461–3482 (2016).
42. Eyring, V. et al. Overview of the Coupled Model Intercomparison Project Phase 6 (CMIP6) experimental design and organization. *Geosci. Model Dev.* **9**, 1937–1958 (2016).
43. Brogli, R., Heim, C., Mensch, J., Sørland, S. L. & Schär, C. The pseudo-global-warming (PGW) approach: methodology, software package PGW4ERA5 v1.1, validation, and sensitivity analyses. *Geosci. Model Dev.* **16**, 907–926 (2023).
44. Niu, G.-Y. et al. The community Noah land surface model with multiparameterization options (Noah-MP): 1. Model description and evaluation with local-scale measurements. *J. Geophys. Res. Atmos.* **116**, D12109 (2011).
45. Juras, R., Blöcher, J. R., Jenicek, M., Hotovy, O. & Markonis, Y. What affects the hydrological response of rain-on-snow events in low-altitude mountain ranges in Central Europe? *J. Hydrol.* **603**, 127002 (2021).
46. Freudiger, D., Kohn, I., Stahl, K. & Weiler, M. Large-scale analysis of changing frequencies of rain-on-snow events with flood-generation potential. *Hydrol. Earth Syst. Sci.* **18**, 2695–2709 (2014).
47. AR5 Climate Change 2013: The Physical Science Basis — IPCC. <https://www.ipcc.ch/report/ar5/wg1/>.
48. AR4 Climate Change 2007: The Physical Science Basis — IPCC. <https://www.ipcc.ch/report/ar4/wg1/>.
49. *Climate Change 2021: The Physical Science Basis. Contribution of Working Group I to the Sixth Assessment Report of the Intergovernmental Panel on Climate Change.* (Cambridge University Press, Cambridge, United Kingdom and New York, NY, USA, 2021). <https://doi.org/10.1017/9781009157896>.
50. Maina, F. Z., Siirila-Woodburn, E. R. & Vahmani, P. Sensitivity of meteorological-forcing resolution on hydrologic variables. *Hydrol. Earth Syst. Sci.* **24**, 3451–3474 (2020).
51. Pflug, J. M., Hughes, M. & Lundquist, J. D. Downscaling snow deposition using historic snow depth patterns: diagnosing limitations from snowfall biases, winter snow losses, and interannual snow pattern repeatability. *Water Resour. Res.* **57**, e2021WR029999 (2021).
52. Bonsoms, J., López-Moreno, J. I., Alonso-González, E., Deschamps-Berger, C. & Oliva, M. Rain-on-snow responses to warmer Pyrenees: a sensitivity analysis using a physically based snow hydrological model. *Nat. Hazards Earth Syst. Sci.* **24**, 245–264 (2024).
53. Tebaldi, C. et al. Climate model projections from the Scenario Model Intercomparison Project (ScenarioMIP) of CMIP6. *Earth Syst. Dyn.* **12**, 253–293 (2021).
54. Davenport, F. V., Herrera-Estrada, J. E., Burke, M. & Diffenbaugh, N. S. Flood size increases nonlinearly across the western United States in response to lower snow-precipitation ratios. *Water Resour. Res.* **56**, e2019WR025571 (2020).
55. Kumar, S. V. et al. Land information system: an interoperable framework for high resolution land surface modeling. *Environ. Model. Softw.* **21**, 1402–1415 (2006).
56. He, C. et al. Modernizing the open-source community Noah with multi-parameterization options (Noah-MP) land surface model (version 5.0) with enhanced modularity, interoperability, and applicability. *Geosci. Model Dev.* **16**, 5131–5151 (2023).
57. Maina, F. & Kumar, S. High mountain asia daily 0.05 x 0.05 deg Noah-MP land surface model reanalysis, Version 1. NASA National Snow and Ice Data Center Distributed Active Archive Center <https://doi.org/10.5067/FCHUV8F5Z8OD> (2023).
58. Liu, X., Chen, F., Barlage, M., Zhou, G. & Niyogi, D. Noah-MP-Crop: introducing dynamic crop growth in the Noah-MP land surface model. *J. Geophys. Res. Atmos.* **121**, 13,953–13,972 (2016).
59. Thrasher, B. et al. NASA Global Daily Downscaled Projections, CMIP6. *Sci. Data* **9**, 262 (2022).
60. Wood, A. W., Leung, L. R., Sridhar, V. & Lettenmaier, D. P. Hydrologic implications of dynamical and statistical approaches to downscaling climate model outputs. *Clim. Change* **62**, 189–216 (2004).
61. Sheffield, J., Goteti, G. & Wood, E. F. Development of a 50-Year high-resolution global dataset of meteorological forcings for land surface modeling. *J. Clim.* **19**, 3088–3111 (2006).
62. Gelaro, R. et al. The modern-era retrospective analysis for research and applications, Version 2 (MERRA-2). *J. Clim.* **30**, 5419–5454 (2017).
63. Muñoz-Sabater, J. et al. ERA5-Land: a state-of-the-art global reanalysis dataset for land applications. *Earth Syst. Sci. Data* **13**, 4349–4383 (2021).
64. Huffman, G. J., Bolvin, D. T. & Nelkin, E. J. Integrated multi-satellite retrievals for GPM (IMERG) technical documentation. *NASAGSFC Code* **612**, 47 (2015).
65. Nie, W. et al. Nonstationarity in the global terrestrial water cycle and its interlinkages in the Anthropocene. *Proc. Natl. Acad. Sci. USA* **121**, e2403707121 (2024).
66. Mazurkiewicz, A. B., Callery, D. G. & McDonnell, J. J. Assessing the controls of the snow energy balance and water available for runoff in a rain-on-snow environment. *J. Hydrol.* **354**, 1–14 (2008).
67. Yan, H. et al. Next-generation intensity-duration-frequency curves for hydrologic design in snow-dominated environments. *Water Resour. Res.* **54**, 1093–1108 (2018).

68. Yoon, Y. et al. Evaluating the uncertainty of terrestrial water budget components over high mountain Asia. *Front. Earth Sci.* **7**, 120 (2019).
69. Maina, F. Z. et al. Development of a multidecadal land reanalysis over High Mountain Asia. *Sci. Data* **11**, 827 (2024).
70. Yue, S., Pilon, P. & Cavadias, G. Power of the Mann–Kendall and Spearman’s rho tests for detecting monotonic trends in hydrological series. *J. Hydrol.* **259**, 254–271 (2002).
71. Kendall, M. G. *Rank Correlation Methods*. (Griffin, Oxford, 1948).
72. Mann, H. B. Nonparametric tests against trend. *Econometrica* **13**, 245–259 (1945).
73. Maina, F., & Kumar, S. Global patterns of rain-on-snow and its impacts on runoff from past to future projections [Data set]. Zenodo. <https://doi.org/10.5281/zenodo.15200067> (2025).

Acknowledgements

Computing was supported by the resources at the NASA Center for Climate Simulation.

Author contributions

F.Z.M. designed the study and methodology, generated the input data, analyzed the data, wrote and edited the manuscript. S.V.K. designed the study, generated the input data, performed simulations, performed model evaluation and validation, and edited the manuscript.

Competing interests

The authors declare no competing interests.

Additional information

Supplementary information The online version contains supplementary material available at <https://doi.org/10.1038/s41467-025-59855-3>.

Correspondence and requests for materials should be addressed to Fadji Z. Maina.

Peer review information *Nature Communications* thanks Xiaodong Chen, Lu Li and the other, anonymous, reviewer(s) for their contribution to the peer review of this work. A peer review file is available.

Reprints and permissions information is available at <http://www.nature.com/reprints>

Publisher’s note Springer Nature remains neutral with regard to jurisdictional claims in published maps and institutional affiliations.

Open Access This article is licensed under a Creative Commons Attribution-NonCommercial-NoDerivatives 4.0 International License, which permits any non-commercial use, sharing, distribution and reproduction in any medium or format, as long as you give appropriate credit to the original author(s) and the source, provide a link to the Creative Commons licence, and indicate if you modified the licensed material. You do not have permission under this licence to share adapted material derived from this article or parts of it. The images or other third party material in this article are included in the article’s Creative Commons licence, unless indicated otherwise in a credit line to the material. If material is not included in the article’s Creative Commons licence and your intended use is not permitted by statutory regulation or exceeds the permitted use, you will need to obtain permission directly from the copyright holder. To view a copy of this licence, visit <http://creativecommons.org/licenses/by-nc-nd/4.0/>.

© The Author(s) 2025